Journal of Fluorine Chemistry 132 (2011) 587–595

Contents lists available at ScienceDirect

Journal of Fluorine Chemistry

journal homepage: www.elsevier.com/locate/fluor

C–F···M$^+$ interaction in anionic α-fluorovinyl rhenium oxycarbene complexes and their β-fluoroenolate analogs

Petr K. Sazonov [a,*], Yuri F. Oprunenko [a], Victor N. Khrustalev [b], Irina P. Beletskaya [a,*]

[a] Chemistry Department of the M.V. Lomonosov Moscow State University, 119992 Moscow, Russia
[b] A.N. Nesmeyanov Institute of Organoelement Compounds (INEOS), Russian Academy of Sciences, Vavilov Street 28, 119991 Moscow, Russia

ARTICLE INFO

Article history:
Received 11 April 2011
Received in revised form 6 June 2011
Accepted 8 June 2011
Available online 15 June 2011

Keywords:
C–F sigma donor
^{19}F NMR
DFT calculations
α-Fluorovinyl enolates
Anionic acyl complexes

ABSTRACT

The C–F···M$^+$ interaction in anionic σ-(α-fluorovinyl)rhenium oxycarbene complexes, [RCF=CFRe=C(O)R′(CO)$_4$]M (**1**–**6**), M = Na, Li, K is studied by ^{19}F NMR in THF and Et$_2$O. The coordination of α-F to M$^+$ results in an upfield shift of the corresponding ^{19}F NMR signal and a decrease of $^1J_{CF}$. The maximum shift is found for the Li salt of complex **4** in Et$_2$O ($\Delta\delta_{F\alpha}$ = 36.4 ppm), in which case a ^{7}Li–^{19}F spin–spin coupling is also observed (J_{LiF} = 40 Hz). The ΔE of C–F···M$^+$ interaction and its effect on ^{19}F shielding was further studied by DFT calculations using β-fluoroenolates as models, which confirmed a strong impact of CF-bond environment on the coordination ability of fluorine in these F,O-chelates. A compound with a β-fluoroenolate backbone but without rhenium, *o*-(α-fluorovinyl)phenolate **12**, was prepared and studied by ^{19}F NMR, and similarly showed indications of C–F···M$^+$ interaction in THF solution. It is concluded that the donor ability of fluorine in the studied system is enhanced because of the conjugation of α-fluorovinyl group with the enolate π-system and back donation from the transition metal.

1. Introduction

The ability of C–F units in organofluorine compounds to act as a hard donor center for metal cations, although obvious, was recognized only in the early 1980s, when Glusker and Murray-Rust et al. pointed to a wide occurrence of short CF···M^{n+} contacts in crystal structures [1]. Hundreds of close CF···M^{n+} contacts have been reported in crystal state, for which the steric crowding and crystal packing effects are largely responsible, however, there are but a few cases, when such contacts persist in solution. Among the notable exceptions are fluorine-containing cage compounds developed by Plenio [2–8] and Takemura [9–13] groups and zirconocenium cations with fluorophenylborate counteranions [3,14–18]. The CF···M^{n+} coordination in cage compounds is achieved through a high degree of donor center preorganization, the encapsulated cation being unable to avoid the interaction with fluorine, which resembles the situation in the crystal state. Apart form these special cases, the CF···M^{n+} interaction in donor solvents, competing with CF units, remains a sort of chemical curiosity, and the requirements for such an interaction are not very well understood. The effect of C–F bond inherent characteristics in different chemical environments has not been evaluated or discussed.

In the reaction of [Re(CO)$_5$]Na with chlorotrifluoroethylene we observed and isolated an anionic oxycarbene complex **1** [19], whose ^{19}F NMR spectrum in THF solution possessed some unexpected dynamic features. In the spectrum of its Na$^+$ salt the resonance of vinylic α-fluorine is broad and appears at an unusually high field, but shifts ~9 ppm downfield to the expected region on the addition of 18-crown-6 to the sample. Such behavior was suggestive of CF···Na$^+$ interaction, which is being confirmed in the present communication by studying the ^{19}F NMR spectra of various α-fluorovinyl oxycarbene rhenium complexes with different singly charged cations (Na, Li, K, Tl). To better understand what makes the CF···M$^+$ interaction feasible in these complexes, additional model systems were studied computationally, and some of them, such as β-fluoroenolates, were synthesized and studied in solution by ^{19}F NMR.

2. Results and discussion

Complex **1** results from the nucleophilic addition of [(CO)$_5$ReCF$_2$CFCl]$^-$ carbanion to the CO ligand of CF$_2$=CFRe(CO)$_5$. The carbanion is in turn formed as an intermediate in the reaction of [Re(CO)$_5$]Na with CF$_2$=CFCl [19]. Nucleophilic attack at the coordinated CO is quite typical for XRe(CO)$_5$ complexes [20–24] and various oxycarbene rhenium anions (**2**–**6**) can be generated

* Corresponding authors. Fax: +7 495 939 3618.
E-mail addresses: pksspk@yandex.ru, petr@elorg.chem.msu.ru (P.K. Sazonov), beletska@org.chem.msu.ru (I.P. Beletskaya).

0022-1139/$ – see front matter © 2011 Elsevier B.V. All rights reserved.
doi:10.1016/j.jfluchem.2011.06.008

Table 1
Cation effects on ^{19}F chemical shifts in rhenium oxycarbene complexes in THF, 22 °C.

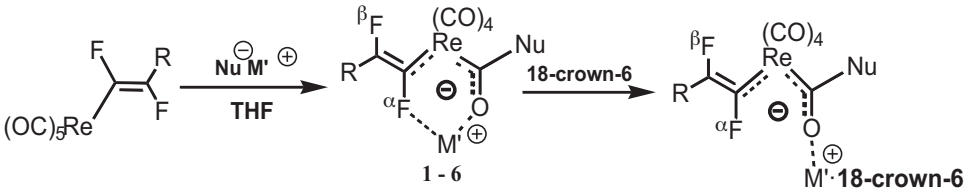

Complex	R	NuM′	$\delta_{F\alpha}$ [a]			$\Delta\delta_{F\alpha}$	$\Delta\delta_{F\beta}$
			Starting $RRe(CO)_5$ [c]	Complex **1–6**	Complex **1–6** + 18-crown-6		
1	F	[b]	−144.5	−156.9	−147.2	9.7	−0.3
2	F	*t*-BuONa	−144.5	−162.7	−146.1	16.6	−1.9
2	F	*t*-BuOK	−144.5	−153.7	−147.8	5.9	−0.4
2	F	*t*-BuOLi	−144.5	−160.9	−147.2[f]	13.7	−1.2
3	$(CF_3)_3C$	*t*-BuONa	−87.0	−99.0	−91.5	7.5	−1.8
4	Ph	*t*-BuONa	−99.4	−111.7	−92.5	19.2	2.2
4[d]	Ph	*t*-BuONa	−99.0	−120.2	−92.5[e]	27.7	−0.6
4[d]	Ph	*t*-BuOLi	−99.0	−132.1	−95.7[e,f]	36.4	−6.4
5	F	[PhC≡C]Na	−144.5	−155.0	−147.8	7.2	−0.5
6	Ph	[PhC≡C]Na	−99.4	−103.3	−98.3	5.0	−0.9

[a] $\Delta\delta_F = \delta_F$ (complex + 18-crown-6) − δ_F (complex).
[b] NuM′ = $[(CO)_5ReCF_2CFCl]Na$.
[c] NMR data from Refs. [19,25,26].
[d] In Et_2O solvent.
[e] In THF.
[f] With [2.2.1]-cryptand.

from (α-fluorovinyl)$Re(CO)_5$ complexes (Table 1). A coordinating solvent (THF or Et_2O) is required for this nucleophilic addition reaction, e.g. *t*-BuONa does not react with $PhCF{=}CFRe(CO)_5$ in toluene, but when 18-crown-6 is added, an instantaneous reaction follows. The formation of anionic oxycarbene complexes is confirmed by characteristic changes in IR and ^1H, ^{19}F and ^{13}C NMR spectra.

Crystals of apparently good quality were obtained for the complex of Na salt of **1** with 18-crown-6 and dioxane which, however, turned out to be mimetic twins unsuitable for X-ray structure determination.

The addition of 18-crown-6 to the solutions of the complexes in THF causes a significant change in their ion pair state, as evidenced by changes in the IR frequencies of Re-coordinated CO groups. All ν(CO) bands are shifted to lower frequencies, which corresponds to a decrease of C≡O bond order resulting from additional charge transfer to the antibonding π* orbitals. In Et_2O solvent the ν(CO) bands are shifted to higher frequencies compared to THF. The lowest frequency ν(CO) band (B_2 mode) is most sensitive to ion-pairing, shifting (in case of complex **4**) from 1944 cm^{-1} (Li, Et_2O) and 1940 cm^{-1} (Na, Et_2O) to 1930 cm^{-1} (Na, THF) and finally to 1908 cm^{-1} (Na + 18-crown-6, THF). Thus, the ion pair separation in the rhenium oxycarbene anions increases on going from Et_2O to THF and then to THF + 18-crown-6, though the contact of alkaline metal cation with the acyl oxygen may remain even in the presence of 18-crown-6.

Formation of oxycarbene anions (**2–6**) from neutral (α-fluorovinyl)$Re(CO)_5$ compounds always results in an upfield shift of α-fluorine resonance in ^{19}F NMR spectrum. The addition of crown ether or cryptand shifts the α-fluorine signal downfield, so that it returns to the values observed for the neutral $Re(CO)_5$ complexes (±3 ppm). The shift of β-fluorine changes only slightly, usually in the opposite direction (Table 1). The upfield shift of the ^{19}F NMR resonance can be qualitatively explained in terms of increased electron density around fluorine which in turn results from cation-induced CF-bond polarization.

Much higher upfield shifts of α-fluorine signal than in more basic solvent, THF, are observed in Et_2O, reaching 36.4 ppm for the Li salt of complex **4**. Moreover, in this case a spin–spin coupling of α-fluorine to lithium (J = 40 Hz) is observed, providing a direct proof of lithium–fluorine interaction. The α-fluorine signal appears as a doublet ($^3J_{F-F}$) of 1:1:1:1 quartets, the quartet splitting corresponding to spin–spin coupling with ^7Li, I = 3/2 (Fig. 1). Both the $J(^7Li, ^{19}F)$ and the cation induced shift are the highest values reported for the lithium–fluorine interaction [3,6,7]. The effect of Li cation is weaker in THF and spin–spin coupling ^7Li–^{19}F is not observed, possibly because of stronger solvation, which results in the observed order of cation-induced shifts Na > Li > K.

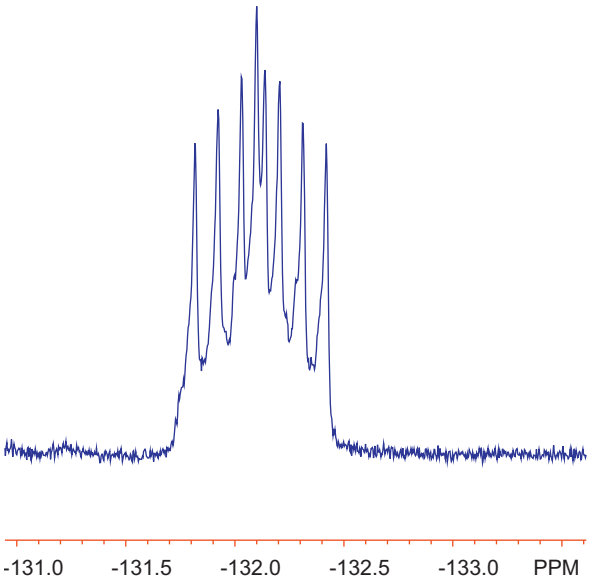

Fig. 1. The multiplet of α-fluorine in the ^{19}F NMR spectrum of the Li salt of complex **4**.

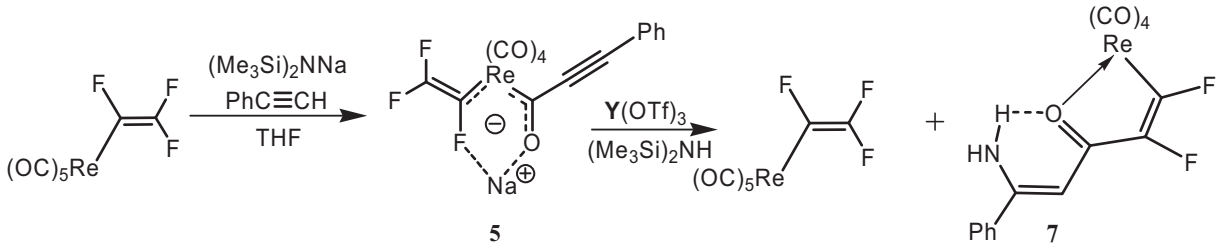

Scheme 1.

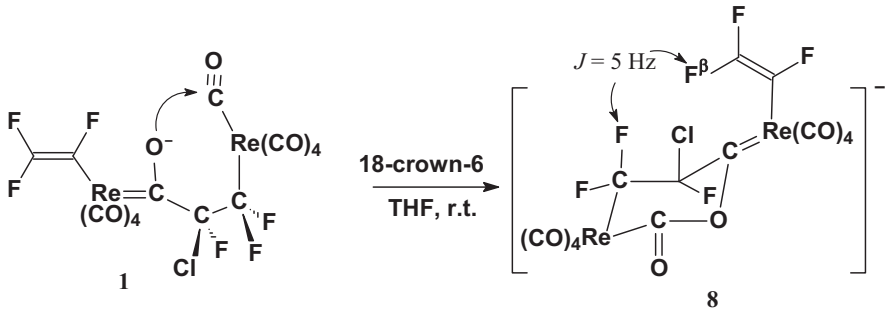

Scheme 2.

A significant decrease of carbon α-fluorine spin–spin coupling constant $^1J_{CF}$ is observed for sodium ($^1J_{CF}$ = 282 Hz) and lithium ($^1J_{CF}$ = 276 Hz) salts of complex **4** in Et_2O, compared to the Li-cryptate salt of the same complex in THF ($^1J_{CF}$ = 300 Hz) or the neutral $Re(CO)_5$ complex ($^1J_{CF}$ = 291 Hz). Decrease of $^1J_{CF}$ is considered as reliable criteria of CF···M^{n+} interaction, being directly related to CF-bond order, which is lowered upon metal coordination to fluorine [3,4,6,9,11,12].

The reaction of sodium salts of complexes **4**, **5** and **6** with $LaCl_3$ or $Y(OTf)_3$ instead of the expected cation exchange resulted in the protonolysis [13], regenerating the neutral (vinyl)$Re(CO)_5$ complex. In the reaction of complex **5** with $Y(OTf)_3$ besides CF_2=CFRe$(CO)_5$ a product of formal CF-activation–CO-insertion (**7**) was isolated (Scheme 1). The amino-group in compound **7** can result from the $(Me_3Si)_2NH$ produced in the metallation reaction of PhC≡CH with $(Me_3Si)_2NNa$.

The rhenium oxycarbene complexes, even in the form of alkaline metal salts, are not very stable in solution. An interesting transformation is observed for complex **1** in the presence of 18-crown-6 in THF, which after several days at room temperature rearranges into a red-colored complex, apparently of a metallocyclic structure **8** (Scheme 2). The IR and ^{13}C NMR spectra of **8** display the patterns of two different $X_2Re(CO)_4$ fragments, and its ^{19}F NMR spectrum the same pattern of signals as that of **1** with slightly different chemical shifts. The observation of a through-space spin–spin coupling between fluorine nuclei F^{β} belonging to CF_2=CF group and one of the fluorine nuclei of CF_2-group is an additional point in favor of a cyclic structure **8**. Complex **8** results from an intramolecular nucleophilic addition of the acyl oxygen to the CO ligand of the $Re(CO)_5$ group (Scheme 2).

The rhenium oxycarbene anions can be regarded as β-diketonate analogs where one oxygen atom is replaced with fluorine (Fig. 2). The persistence of CF···M^+ interaction in donor solvents (THF) can thus be attributed to chelate effect. The electron density on fluorine is increased due to conjugation of the fluorine lone pair with negatively charged enolate system, which enhances its donor properties.

However, the oxycarbene rhenium complexes **9** and **10** [23], though they have a similar conjugated F,O-chelate system, display no signs of cation–fluorine interaction (Fig. 3). The corresponding fluorine (β) signal is shifted only slightly and to higher field upon the addition of crown ether.

Thus the electronic environment of C–F bond seems to play an important role in determining its coordination ability. To gain a further insight into the C–F interaction in such chelate systems we performed a computational model study. The sign of the cation-induced ^{19}F chemical shift ($\Delta\delta_F$) was the first question considered. For different ligands/cations both negative (high filed) [5–7] and positive values [5,27] are reported in the literature, allowing one to question the reliability of $\Delta\delta_F$ as an indicator of CF···M^{n+} interaction.

Fluorovinylenolates were chosen as models of rhenium oxycarbene complexes to simplify the calculation. In sodium 3,4,4-trifluoro-1,3-dien-1-olat, taken as a first model compound, the CF···Na^+ coordination is possible only in *Z*-isomer. Both at MP2

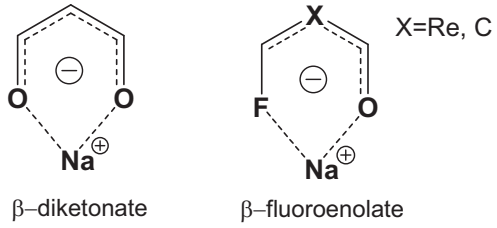

Fig. 2. Analogy between β-diketonates and rhenium oxycarbene anions (β-fluoroenolates).

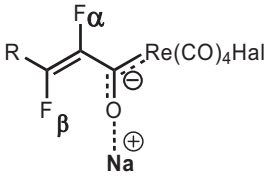

9 R = F, Hal=Br
10 R= $(CF_3)_3C$, Hal=Cl

The effect of 18-crown-6:

$\Delta\delta_{F_\alpha}$~1 ppm

$\Delta\delta_{F_\beta}$~ −(3–5) ppm

Fig. 3. Oxycarbene rhenium complexes without CF···Na^+ interaction.

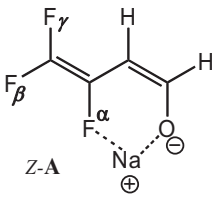

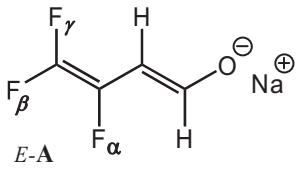

Method	$\delta_{F\alpha}$	$\delta_{F\beta}$	$\delta_{F\gamma}$	$\delta_{F\alpha}$	$\delta_{F\beta}$	$\delta_{F\gamma}$
MP2/6-311+G(d)	-155.5	-108.1	-121.0	-142.0	-106.3	-124.6
B3LYP/6-31+G(d)	-150.0	-103.9	-113.0	-135.0	-98.5	-117.35

Fig. 4. Computed ^{19}F NMR chemical shifts (δ_F) in *Z*- and *E*-isomers of sodium 3,4,4-trifluoro-1, 3-dien-1-olate.

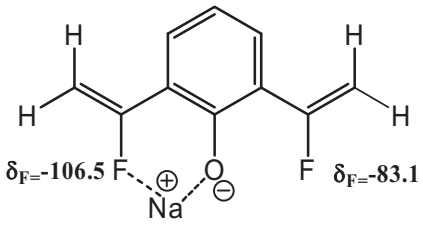

B B3LYP/6-31+G(d)

Fig. 5. Computed values of δ_F in 2,6-bis(α-fluorovinyl)phenolate.

and DFT theory levels, the sodium coordinated fluorine in the *Z*-isomer is more shielded (by ~15 ppm) than the non-coordinated one in the *E*-isomer (Fig. 4).

The second model structure, 2,6-bis(α-fluorovinyl)phenolate (Fig. 5), allows to compare ^{19}F chemical shifts of otherwise identical fluorovinyl groups one of which is coordinated to sodium. In this model the interaction with sodium also shields the corresponding ^{19}F nuclei ($\Delta\delta_F$ = 23.4 ppm).

In fact the increased ^{19}F shielding upon sodium cation coordination is observed in all model systems examined (Table 2), and hence it can be considered a reliable experimental criteria of CF···Na^+ coordination.

The distance CF···Na^+ is an important characteristic of CF-metal interaction. As can be seen from the data in Table 2, the shortest CF···Na^+ distances are calculated for the interaction of internal

Table 2
Some properties of model F,O-chelates calculated by B3LYP/6-31+G(d) method.

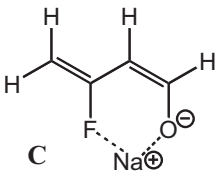

C

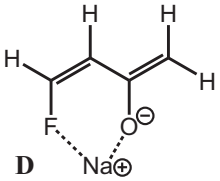

D

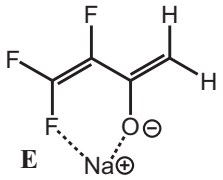

E

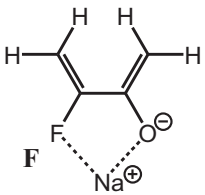

F

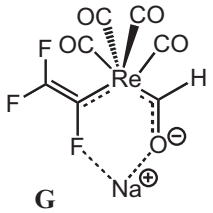

G

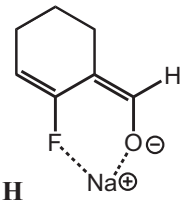

H

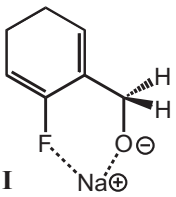

I

.

Model	Chelate cycle	*d*(C–F) non-coord., Å[a]	*d*(CF···Na^+), Å	*d*(CO···Na^+), Å	C–F···Na^+ angle, °	ΔE(CF···Na^+), kcal/mol[b]	$\Delta\delta_F$[c]
Z–**A**	Twisted	1.382	2.192	2.098	110.4	−9.9	15.0
C	Flat	1.388	2.160	2.079	130.5	−10.9	21.8
D	Flat	1.373	2.214	2.042	123.6	−6.4	28.5
E	Flat	1.339	2.313	2.028	125.4	−2.6	23.0
F	Twisted	1.376	2.249	2.071	110.1	−5.7	21.5
G[d]	Twisted	1.400	2.199	2.157	90.3	−18.4	16.3
H	Flat	1.386	2.158	2.074	128.1	−10.8	20.0
I	Twisted	1.368	2.298	2.049	113.2	−3.9	16.5

[a] In a structure with a linearly constrained C–O···Na angle, which breaks the CF···Na^+ contact.
[b] ΔE(CF···Na^+) is calculated as a difference in energy between the fully optimized structure and the structure with a linearly constrained C–O···Na angle.
[c] Calculated similarly to ΔE, $\Delta\delta_F = \delta_F($ 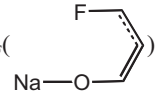 $) - \delta_F($ 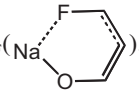 $)$.
[d] SDD basis set with effective core potentials used for rhenium [28].

α-fluorine with cation in six-membered F,O-chelates (structures *Z*–**A**, **C** and **H**). The interaction with terminal β-fluorine (**D**, **E**) or in a five-membered chelate cycle (**F**) is characterized by longer CF···Na^+ distances. There is also a tendency towards shorter CF···Na^+ distances in flat F,O-chelates (compare *Z*–**A** and **C**). The planarity of the chelate cycle also governs the angle C–F···Na^+, which is smaller for twisted F,O-chelates (90.3–113.2°) than for flat ones (123.6–130.5°). The distances CO···Na^+ are expectedly shorter than CF···Na^+, the difference being small for Re-oxycarbene structure **G** and considerable for all its β-fluoroenolate analogs.

To compare the energetics of CF···Na^+ interaction each of the model structures was reoptimized with a C–O···Na angle fixed to 180°, which breaks the CF···Na^+ contact. As can be seen from the data in Table 2, the highest energy gain upon CF···Na^+ coordination is calculated for internal α-fluorine (*Z*–**A** and **C**), exactly the type of fluorine that is coordinated in the rhenium complexes **1**–**6**. Terminal β-fluorine (**D**), especially in a CF_2-group (**E**), is predicted to be a much weaker donor center, as is the α-fluorine in a 5-member chelate cycle (**F**). It should be pointed out that only these latter less favorable fluorine coordination modes are available in rhenium complexes **9** and **10**, and it is not surprising that CF···Na coordination is actually not observed.

The computed energy of CF···Na interaction correlates with the length of the corresponding CF-bond in the non-coordinated state. In other words, the longer and consequently weaker CF-bonds are better σ-donors. It was illuminating to find in Cambridge Crystal Data Base [29] that the longest fluorine to sp^2-carbon bonds (0.138–0.140 nm) occur in α-fluorovinyl transition metal compounds. The α-CF group in oxycarbene rhenium complexes is therefore a better σ-donor than the corresponding group in fluorovinylenolates. This conclusion is confirmed by the calculation performed for a rhenium oxycarbene complex (G), for which an unusually long C–F bond is predicted. The stabilization energy associated with its interaction with sodium is significantly higher than in all fluovinylenolate models. This effect of rhenium can be interpreted in terms of high back-donating ability of 18-e transition metal center.

The success of using fluoroenolates for computational modeling of CF···Na interaction suggests that such interactions in β-fluoroenolates could be observed experimentally. However, facile β-fluoride elimination is a serious obstacle for the generation and NMR study of β-fluoroenolates [30]. An attempt to prepare the sodium salt of α-fluorovinyl enolate from the (*E*)-3,4-difluoro-1,4-diphenylbut-3-en-1-one gave only the corresponding allene as the only identifiable product. As a bypass solution we decided to use in place of β-fluoroenolate an *o*-(α-fluorovinyl)phenolate, which has the structural motif needed for the formation of 6-memberd F,O-chelate, but is a stable compound.

The structure of the parent (*E*)-2-(1,2-difluoro-2-phenylvinyl)-phenol (**11**) was established by the single-crystal X-ray diffraction analysis of its 2:1 adduct with diaza-18-crown-6 (Fig. 6). The molecule of **11** is non-planar. The phenolic and phenyl moieties are twisted relative to the central difluoroethylenic fragment by 48.1 and 23.2°, respectively, due to steric reasons (the intramolecular repulsive interactions between the hydrogen and fluorine atoms – H14···F1 and H8···F2). The larger value of the dihedral angle observed in the case of the phenolic moiety is apparently explained by the intermolecular O1–H1O···N1 hydrogen bond with the diaza-18-crown-6 molecule (O···N 2.711(3) Å, H···N 1.81 Å, ∠O–H···N 171°, Fig. 6).

There is evidence of an intramolecular hydrogen bond to fluorine in phenol **11**. The ^{1}H NMR signal of the phenolic hydrogen shows a triplet splitting (J_{HF} = 5 Hz) in $CDCl_3$ solution, but the splitting is removed and the signal shifted by 3 ppm to lower field in THF, as a result of stronger hydrogen bonding to THF oxygen [31].

The α-fluorine ^{19}F NMR signal of sodium (*E*)-2-(1,2-difluoro-2-phenylvinyl)phenolate (**12**) is broad. Upon the addition of 18-crown-6 the signal is narrowed and shifts downfield (Table 3, en. 1), a behavior characteristic of CF···Na^+ interaction. As expected for cation-induced shift the effect of crown ether is more pronounced in toluene, a less polar solvent, (Table 3, en. 2). Other singly charged cations also produce an upfield shift of α-fluorine signal, since the addition of 18-crown-6 or cryptand shifts the signal downfield. The effect is smaller than observed for Na, which can be explained either by decreased charge density (K, Tl) or by stronger solvation (Li). Unfortunately, despite considerable effort involving low temperature measurements, no ^{203,205}Tl–^{19}F spin–spin coupling constant [10,13] was observed in ^{19}F NMR spectrum.

Thus, the presence of rhenium is not obligatory for CF···M^+ interaction in a conjugated system such as β-fluoroenolate,

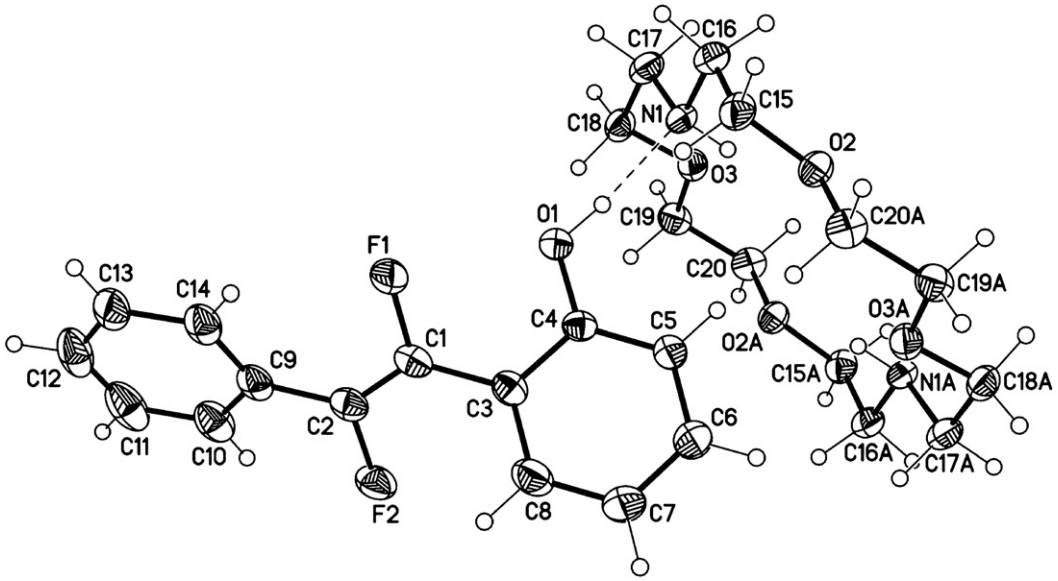

Fig. 6. Molecular structure of adduct of **11** with diaza-18-crown-6 (40% ellipsoids). The dashed line indicates the intermolecular O–H···N hydrogen bond.

Table 3
Cation effects on ^{19}F chemical shifts in (*E*)-2-(1,2-difluoro-2-phenylvinyl)phenolates.

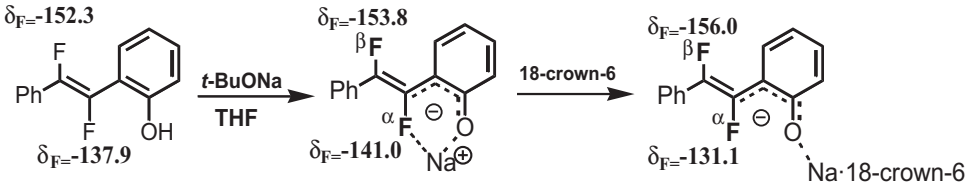

12

Entry	Solvent	Cation	Complexing agent	$\delta_{F\alpha}$		$\Delta\delta_{F\alpha}$[a]	$\Delta\delta_{F\beta}$[a]
				Phenolate	Phenolate + 18-crown-6		
1	THF	Na	18-crown-6	−141.0	−131.1	9.9	−2.2
2	Toluene	Na	18-crown-6	−143.6	−131.4[b]	12.2	−2.8
3	THF	Li	[2.2.1]-cryptand	−139.1[b]	−133.1	6	−0.4
4	THF	K	18-crown-6	−136.3	−131.6	4.7	−1.9
5	THF	Tl	–	−134.9[b]		~4.5[c]	

[a] $\Delta\delta_F = \delta_F$ (anion + 18-crown-6) − δ_F (anion).
[b] Broad signal.
[c] The δ_F of potassium phenolate + 18-crown-6 is taken as a reference.

though the effects observed in ^{19}F NMR spectra of rhenium oxycarbene complexes are more pronounced. But does the conjugation (Fig. 2) really facilitate the CF···M^+ interaction in these systems?

To answer this question two additional model compounds were studied computationally (Table 2), and the stabilization energy of CF···Na^+ interaction was compared for conjugated (**H**) and non-conjugated (**I**) F,O-chelate. The structures were chosen so as to minimize the difference in non-valent interactions in conjugated and non-conjugated systems, while maintaining a similar environment around the α-fluorovinyl group, which in both cases is attached to sp^2-carbon. Interaction energy CF···Na^+ for conjugated F,O-chelate (**H**) falls in the range previously found for similar models *Z*–**A** and **C** (~10 kcal/mol), while for the non-conjugated chelate (**I**) it is less than half of the above value.

Additionally, the role of conjugation in F,O-chelates was proved experimentally, by measuring the ^{19}F NMR spectrum of sodium 1-(2-fluorophenyl)ethoxide. No change of δ_F or of $^1J_{CF}$ was observed upon the addition of 18-crown-6, demonstrating that in a non-conjugated ligand the fluorine does not interact with Na^+ in THF solution.

In flat F,O-chelates, such as models **C**, **D** and **H** (Table 2), the conjugation can be regarded as an antibonding interaction between fluorine lone pair and the π-system of the enolate. However, if the chelate cycle is twisted (as in **A**, **B** and **G**) the negative hyperconjugation of fluorine can also be important.

3. Conclusions

A strong CF···M^+ interaction, which is not broken in THF donor solvent, is found in rhenium σ-fluorovinyl oxycarbene complexes as well as in the analogous *o*-(α-fluorovinyl)phenolate. The present study reveals the factors, which make it feasible, and hence are important for CF···M^+ interaction in general. The negative charge of the ligand (i) and the chelate effect (ii), though important, are not sufficient conditions. The conjugation of the α-fluorovinyl group with the enolate π-system (iii) and its direct connection to transition metal (iv) are the two additional factors, which weaken the CF-bond and increase the donor ability of fluorine.

4. Experimental details

All NMR spectra were recorded on a Varian VXR-400 or a Bruker Avance spectrometer at ambient temperature, ^{19}F NMR at 376.3 MHz using C_6F_6 (δ_F −162.9 ppm) as external or internal standard. ^1H NMR (400.13 MHz) and ^{13}C NMR (100.61 MHz) were referenced to the signals of the solvent. IR spectra were recorded using UR-20 or Thermo-Nicolet IR-200 FT-IR spectrophotometer in a 0.02 cm CaF_2 cell. Trifluorostyrene, σ-(α-fluorovinyl)Re(CO)$_5$ complexes and the anionic rhenium oxycarbene complexes **1**, **9** and **10** were available from the previous studies [19,25,26]. 1-(2-Fluorophenyl)ethanol was obtained by the $NaBH_4$ reduction of *o*-fluoroacetophenone (Aldrich).

4.1. Formation of rhenium oxycarbene complexes 2–6

Reactions were carried out in a small (~5–10 ml) glass vessel with two fused thin-walled NMR tubes (~3.5 mm diameter) under vacuum or argon. The vessel was charged with RCF=CFRe(CO)$_5$ (0.1 mmol), *t*-BuONa (0.12 mmol) or other appropriate base (Table 1). PhC≡CNa was generated from [$(Me_3Si)_2$N]Na and PhC≡CH. THF or Et_2O solvent (0.6–0.8 ml) was vacuum-transferred to the vessel. After warming to r.t. and dissolving the reagents, a part (~0.3 ml) of the reaction solution was decanted to the first NMR tube, which was sealed off with flame. 18-Crown-6 (0.1 mmol, 26 mg) or [2.2.1]-cryptand (0.06 mmol, 20 mg) was added to the rest of the solution, which was transferred to second NMR tube. The sealed tubes we placed inside standard 5 mm NMR tubes containing acetone-d_6 for the lock signal and C_6F_6 for ^{19}F chemical shift reference. Oxycarbene anionic complexes were formed almost quantitatively according to IR, ^1H and ^{19}F NMR spectra, except for the Li salt of complex **4** in Et_2O, which was present in solution together with the unreacted PhCF=CFRe(CO)$_5$ in ~1:1 ratio, even despite using 3 equivalents of *t*-BuOLi.

σ-[3-(Pentacarbonylrhenio)-2,3,3-trifluoro-2-chloropropanoyl]-σ-(trifluorovinyl)tetracarbonylrhenate (**1**) *sodium salt, [CF_2=CFRe(CO)$_4$C(O)CFClCF_2Re(CO)$_5$]Na.* ^{19}F NMR (THF): δ −55.6 (d, br., 1F, $^2J_{FF}$ = 295 Hz); −63.7 (d, br., 1F, $^2J_{FF}$ = 295 Hz); −91 (m, br., 1F); −95.7 (dd, 1F, $^2J_{FF}$ = 98 Hz, $^3J_{FF}$ = 30 Hz); −126.4 (dd, 1F, $^2J_{FF}$ = 98 Hz, $^3J_{FF}$ = 108 Hz); −156.9 (dd, br., 1F, $^3J_{FF}$ = 30 Hz, $^3J_{FF}$ = 108 Hz). ^{19}F NMR (THF + 18-crown-6): δ −57.3 (d, br., 1F, $^2J_{FF}$ = 290 Hz); −62.0 (m, br., 1F); −97.1 (dd, 1F, $^2J_{FF}$ = 98 Hz,

$^3J_{FF}$ = 30 Hz); −113 (m, br., 1F); −126.7 (dd, 1F, $^2J_{FF}$ = 99 Hz, $^3J_{FF}$ = 111 Hz); −147.2 (dd, 1F, $^3J_{FF}$ = 30 Hz, $^3J_{FF}$ = 111 Hz). ^{13}C NMR (THF + 18-crown-6): δ 252.2 (dm, 1C, J_d ~45 Hz); 193.9 (t, 1C, J_{CF} ~6 Hz); 192.4 (t, 1C, J_{CF} ~3 Hz); 191.7 (d, 1C, J_{CF} ~8 Hz); 191.1 (m, 1C); 183.2 (t, 5C, J_{CF} ~6 Hz); the weaker signals of fluorinated backbone were not observed. IR (THF + 18-crown-6): ν 1605 (m, br.) C=O; 1695 (m) C=C; 1920 (vs), 1963 (sh), 1977 (vs), 2028 (vs), 2080 (s), 2142 (m) C≡O.

σ-(Tert-butoxycarbonyl)-σ-(trifluorovinyl)tetracarbonylrhenate (**2**) *[t-BuO(CO)Re(CO)$_4$CF=CF$_2$]M. Sodium salt, M = Na.* ^{19}F NMR (THF): δ −94.6 (dd, 1F, $^2J_{FF}$ = 97 Hz, $^3J_{FF}$ = 30 Hz); −126.0 (dd, 1F, $^2J_{FF}$ = 97 Hz, $^3J_{FF}$ = 106 Hz); −162.7 (dd, 1F, $^3J_{FF}$ = 29 Hz, $^3J_{FF}$ = 106 Hz). IR (THF): ν 1600 (m, br.) C=O; 1690 (m) C=C; 1931 (vs), 1965 (sh), 1975 (vs), 2082 (m) C≡O. ^{19}F NMR (THF + 18-crown-6): δ −95.5 (dd, 1F, $^2J_{FF}$ = 99 Hz, $^3J_{FF}$ = 29 Hz); −125.7 (dd, 1F, $^2J_{FF}$ = 99 Hz, $^3J_{FF}$ = 110 Hz); −146.1 (dd, 1F, $^3J_{FF}$ = 29 Hz, $^3J_{FF}$ = 110 Hz). *Potassium salt, M = K.* ^{19}F NMR (THF): δ −96.1 (dd, 1F, $^2J_{FF}$ = 99 Hz, $^3J_{FF}$ = 29 Hz); −126.5 (dd, 1F, $^2J_{FF}$ = 99 Hz, $^3J_{FF}$ = 108 Hz); −153.7 (dd, 1F, $^3J_{FF}$ = 29 Hz, $^3J_{FF}$ = 108 Hz). IR (THF): ν 1600 (m, br.) C=O; 1690 (m) C=C; 1925 (vs), 1965 (sh), 1975 (vs), 2080 (m) C≡O. ^{19}F NMR (THF + 18-crown-6): δ −96.5 (dd, 1F, $^2J_{FF}$ = 99 Hz, $^3J_{FF}$ = 29 Hz); −126.9 (dd, 1F, $^2J_{FF}$ = 99 Hz, $^3J_{FF}$ = 110 Hz); −147.8 (dd, 1F, $^3J_{FF}$ = 29 Hz, $^3J_{FF}$ = 110 Hz). *Lithium salt, M = Li.* ^{19}F NMR (THF): δ −94.4 (dd, 1F, $^2J_{FF}$ = 96 Hz, $^3J_{FF}$ = 28 Hz); −125.6 (dd, 1F, $^2J_{FF}$ = 96 Hz, $^3J_{FF}$ = 105 Hz); −160.9 (br, 1F). ^{19}F NMR (THF + 2.2.1-cryptand): δ −95.7 (dd, 1F, $^2J_{FF}$ = 98 Hz, $^3J_{FF}$ = 30 Hz); −126.4 (dd, 1F, $^2J_{FF}$ = 98 Hz, $^3J_{FF}$ = 111 Hz); −147.2 (dd, 1F, $^3J_{FF}$ = 30 Hz, $^3J_{FF}$ = 111 Hz).

σ-(Tert-butoxycarbonyl)-σ-(1,2,4,4,4-pentafluoro-3,3-bis(trifluoromethyl)pentenyl)-tetracarbonylrhenate sodium salt (**3**), [*t*-BuO(CO)Re(CO)$_4$CF=CFC(CF$_3$)$_3$]Na. ^{19}F NMR (THF): δ −62.7 (dd, 9F, J_{FF} = 18 Hz, J_{FF} = 14 Hz); −99.0 (br., 1F); −147.7 (d, br., 1F, $^3J_{FF}$ = 130 Hz). ^{19}F NMR (THF + 18-crown-6): δ −62.7 (dd, 9F, J_{FF} = 18 Hz, J_{FF} = 13 Hz); −91.5 (dm, 1F, $^3J_{FF}$ = 127 Hz, $^6J_{FF}$ = 18 Hz); −149.5 (dm, 1F, $^3J_{FF}$ = 127 Hz, $^5J_{FF}$ = 13 Hz).

σ-(Tert-butoxycarbonyl)-σ-(1,2-difluoro-2-phenylethenyl)-tetracarbonylrhenate (**4**), [*t*-BuO(CO)Re(CO)$_4$CF=CFPh]M. *Sodium salt, M = Na.* ^{19}F NMR (THF): δ −111.7 (d, 1F, $^3J_{FF}$ = 109 Hz); −143.9 (d, 1F, $^3J_{FF}$ = 109 Hz). IR (THF): ν 1590 (m, br.) C=O; 1930 (s), 1958 (s), 1977 (vs), 2081 (m) C≡O. ^{19}F NMR (THF + 18-crown-6): δ −92.5 (d, 1F, $^3J_{FF}$ = 112 Hz); −141.7 (d, 1F, $^3J_{FF}$ = 112 Hz). IR (THF + 18-crown-6): ν 1615 (m, br.) C=O; 1908 (s), 1951 (s), 1971 (vs), 2077 (m) C≡O. ^{1}H NMR (Et$_2$O): δ 7.61 (d, 2h); 7.33 (t, 2H); 7.18 (t, 1H); 1.46 (s, 9H). ^{19}F NMR (Et$_2$O): δ −120.2 (d, 1F, $^3J_{FF}$ = 110 Hz); −141.1 (d, 1F, $^3J_{FF}$ = 110 Hz). IR (Et$_2$O): ν 1575 (m, br.) C=O; 1940 (vs), 1968 (s), 1984 (vs), 2081 (m) C≡O. ^{13}C NMR (Et$_2$O): δ 207.5 (s, 1C); 192.0 (d, 1C, J_{CF} = 8 Hz); 191.6 (t, 2C, J_{CF} = 7 Hz); 190.8 (d, 1C, J_{CF} = 5 Hz); 180.6 (dd, $^1J_{CF}$ = 282 Hz, $^2J_{CF}$ = 106 Hz); 160.9 (dd, $^1J_{CF}$ = 204 Hz, $^2J_{CF}$ = 42 Hz); 133.1 (d, $^2J_{CF}$ = 30 Hz); 128.6 (s); 126.8 (s); 125.4 (dd, J_{CF} = 10 Hz, J_{CF} = 7 Hz); 77.4 (s); 29.6 (s). *Lithium salt, M = Li.* ^{1}H NMR (Et$_2$O): δ 7.57 (d, 2h); 7.33 (t, 2H); 7.19 (t, 1H); 1.48 (s, 9H). ^{19}F NMR (Et$_2$O): δ −132.1 (m, 1F, $^3J_{FF}$ = 106 Hz, J_{LiF} = 40 Hz); −138.5 (d, 1F, $^3J_{FF}$ = 106 Hz). ^{13}C NMR (Et$_2$O): δ 210.9 (s, 1C); 192.2 (d, 1C, J_{CF} = 8 Hz); 191.8 (t, 2C, J_{CF} = 6 Hz); 190.9 (d, 1C, J_{CF} = 8 Hz); 180.5 (dd, $^1J_{CF}$ = 276 Hz, $^2J_{CF}$ = 105 Hz); 162.9 (dd, $^1J_{CF}$ = 207 Hz, $^2J_{CF}$ = 45 Hz); 133.9 (d, $^2J_{CF}$ = 30 Hz); 129.2 (s); 128.0 (s); 127.0 (t, J_{CF} = 7 Hz); 79.2 (s); 30.4 (s). IR (Et$_2$O): ν 1560 (m, br.) C=O; 1944 (s), 1967 (s), 1986 (vs), 2082 (s) C≡O. ^{1}H NMR (THF + 2.2.1-cryptand): δ 7.58 (d, 2h); 7.20 (t, 2H); 7.00 (t, 1H); 1.35 (s, 9H). ^{19}F NMR (THF + 2.2.1-cryptand): δ −95.7 (d, 1F, $^3J_{FF}$ = 112 Hz, $^1J_{CF}$ = 300 Hz); −144.9 (d, 1F, $^3J_{FF}$ = 112 Hz); $^1J_{CF}$ measured in ^{13}C satellite.

σ-(3-Phenylpropyn-2-oyl)-σ-(trifluorovinyl)tetracarbonylrhenate sodium salt (**5**), *[PhC≡C(CO)Re(CO)$_4$CF=CF$_2$]Na.* ^{19}F NMR (THF): δ −95.4 (dd, 1F, $^2J_{FF}$ = 97 Hz, $^3J_{FF}$ = 30 Hz); −126.4 (dd, 1F, $^2J_{FF}$ = 97 Hz, $^3J_{FF}$ = 109 Hz); −155.0 (dd, 1F, $^3J_{FF}$ = 30 Hz, $^3J_{FF}$ = 109 Hz). IR (THF): ν 1692 (m) C=C; 1928 (s), 1972 (vs), 2081 (m) C≡O; 2160 (w) C≡C. ^{19}F NMR (THF + 18-crown-6): δ −96.4 (dd, 1F, $^2J_{FF}$ = 98 Hz, $^3J_{FF}$ = 30 Hz); −126.9 (dd, 1F, $^2J_{FF}$ = 98 Hz, $^3J_{FF}$ = 110 Hz); −147.8 (dd, 1F, $^3J_{FF}$ = 30 Hz, $^3J_{FF}$ = 110 Hz).

σ-(3-Phenylpropyn-2-oyl)-σ-(1,2-difluoro-2-phenylethenyl)tetracarbonylrhenate sodium salt (**6**), *[PhC≡C(CO)Re(CO)$_4$CF=CFPh]Na.* ^{19}F NMR (THF): δ −102.9 (d, 1F, $^3J_{FF}$ = 112 Hz); −145.0 (d, 1F, $^3J_{FF}$ = 112 Hz). IR (THF): ν 1594 (m, br.) C=O; 1925 (vs), 1968 (sh), 1973 (vs), 2078 (s) C≡O; 2160 (w, br.) C≡C. ^{19}F NMR (THF + 18-crown-6): δ −97.9 (d, 1F, $^3J_{FF}$ = 112 Hz); −145.9 (d, 1F, $^3J_{FF}$ = 112 Hz).

4.2. Isolation of μ-(5-phenyl-5-amino-3-oxopentadien-1,4-yl-1κC^1:1κO)teracarbonylrhenium (7),

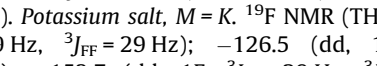

A solution of CF_2=CFRe(CO)$_5$ (100 mg, 0.245 mmol) in 0.5 ml THF was added to a suspension of PhC≡CNa in 1 ml THF, prepared in a Schlenk flask from [(Me$_3$Si)$_2$N]Na (46 mg, 0.25 mmol) and PhC≡CH (27 mg, 0.26 mmol). Samples of the reaction solution were taken for the NMR and IR analysis and to the rest of it solid Y(OTf)$_3$ (64 mg, 0.122 mmol) was added under stirring in two portions, a sample for IR and NMR being taken in between and after the addition of the second portion. IR spectrum indicated the presence of CF_2=CFRe(CO)$_5$ band (2147 cm^{-1}), and two new bands (2107 and 2099 cm^{-1}), the latter subsequently identified as belonging to **7**. Reaction mixture was diluted with CH_2Cl_2 (3 ml) and filtered through an alumina pad. Part of the reaction mixture was separated on a Silufol UV-254 TLC plate, using a CH_2Cl_2–petroleum ether, 1:5 as an eluent. The second yellow band (R_f = 0.3) after solvent removal afforded 4 mg of complex **7** as a yellow solid. ^{1}H NMR (acetone-d_6): δ 9.67 (s, br, 1H, NH); 8.26 (s, br, 1H, NH); 7.78 (d, 2h); 7.62 (t, 1H); 7.55 (t, 2H); 5.63 (t, 1H, J_{HF} = 2.7 Hz); 1.48 (s, 9H). ^{19}F NMR (Et$_2$O): δ −70.4 (m, 1F); −141.6 (m, 1F). IR (THF): ν 1544 (s) C=O; 1941 (vs), 1985 (sh), 1996 (vs), 2099 (s) C≡O. EIMS (direct inlet) 70 eV, *m/z* (rel. int.): 507 [M]$^+$ (10), 479 [M−CO]$^+$ (10), 451 [M−2CO]$^+$ (20), 423 [M−3CO]$^+$ (10), 395 [M−4CO]$^+$ (30), 103 [PhC$_2$H$_2$]$^+$ (100).

4.3. Spectral data for complexes 8–10

μ-(1,1,2-Trifluoro-2-chloro-4-oxa-5-oxopentyliden-2κC^3-diyl-1κC^1:1κC^5)trifluorovinyl-2κC-octacarbonyl-1κ^{4}C,2κ^{4}C-dirhenate

(-1) sodium (**8**), 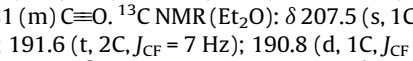 ^{19}F NMR (THF-d_8 + 18-crown-6): δ −68.4 (dt, 1F, $^2J_{FF}$ = 281 Hz, J_t = 5 Hz); −85.1 (dd, 1F, $^2J_{FF}$ = 281 Hz, $^3J_{FF}$ = 6 Hz); −94.9 (dd, 1F, $^2J_{FF}$ = 96 Hz, $^3J_{FF}$ = 31 Hz); −124.6 (t, 1F, J_t = 6 Hz); −125.5 (ddd, 1F, $^2J_{FF}$ = 96 Hz, $^3J_{FF}$ = 111 Hz, $^8J_{FF}$ = 5 Hz); −146.6 (dd, 1F, $^3J_{FF}$ = 31 Hz, $^3J_{FF}$ = 111 Hz). ^{13}C NMR (THF-d_8 + 18-crown-6): δ 290.2 (dm, J_d = 50 Hz); 199.2 (br, 1C); 192.8 (d, 1C); 192.0 (m, 1C); 191.6 (m, 1C); 191.3 (m, 1C); 190.9 (t, 1C, J_{CF} = 3.5 Hz); 188.9 (m, 1C, J_{CF} = 10 Hz); 188.3 (m, 1C); 188.0 (d, 1C, J_{CF} = 21 Hz); the weaker signals of fluorinated backbone were not observed. IR (THF + 18-crown-6): ν 1697 (m) C=C; 1933 (vs), 1943 (sh), 1988 (vs), 1998 (vs), 2088 (s), 2100 (m) C≡O.

Bromo-σ-(3,3,2-trifluoropropen-2-oyl)tetracarbonylrhenate sodium salt (**9**), *[CF$_2$=CF(CO)Re(CO)$_4$Br]Na.* ^{19}F NMR (THF + 18-crown-6): δ −105.5 (t, 1F, J_{FF} = 35 Hz); −111.1 (dd, 1F, $^2J_{FF}$ = 36 Hz, $^3J_{FF}$ = 110 Hz); −160.4 (dd, 1F, $^3J_{FF}$ = 34 Hz, $^3J_{FF}$ = 110 Hz).

Chloro-σ-(2,3,5,5,5-pentafluoro-4,4-bis(trifluoromethyl)penten-2-oyl]tetracarbonylrhenate sodium salt (**10**), *[(CF$_3$)$_3$CCF=CF(CO)R-*

CF(CO)Re(CO)$_4$Cl]Na. ^{19}F NMR (THF + 2.2.2-cryptand): δ −61.9 (dd, 9F, J_{FF} = 17 Hz, J_{FF} = 13 Hz); −128.2 (dm, 1F, $^3J_{FF}$ = 133 Hz, $^6J_{FF}$ = 17 Hz); −169.9 (dm, 1F, $^3J_{FF}$ = 133 Hz, $^5J_{FF}$ = 12 Hz). Spectral data for complexes **9** and **10** without 18-crown-6 or cryptand is given in Ref. [23].

4.4. Synthesis of (E)-2-(1,2-difluoro-2-phenylvinyl)phenol (11), (o-OHC$_6$H$_4$)CF=CFPh, and of the corresponding phenolates

A solution of BuLi (5 mmol) in 2 ml of petroleum ether was added dropwise to a stirred solution of o-BrC$_6$H$_4$OH (430 mg, 2.5 mmol) in THF (5 ml) at −60 °C under argon atmosphere. The reaction mixture was allowed to warm to r.t. and stirred for 3 hr. PhCF=CF$_2$ (440 mg, 2.78 mmol) was added dropwise to the resulting clear solution and the reaction mixture was left stirring overnight. After aqueous HCl workup, extraction with CH_2Cl_2 (2 × 5 ml) and solvent removal the residue was separated by column chromatography on silica gel (Merk, 35–70 mkm). The first fraction gave after solvent removal (*o*-OHC$_6$H$_4$)CF=CFPh product (200 mg, 0.86 mmol) as a colorless solid. ^{1}H NMR ($CDCl_3$): δ 7.80 (d, 2h); 7.35–7.53 (m, 5H); 7.05 (m, 2H); 5.60 (t, 1H, J_{HF} = 5 Hz, O*H*). ^{1}H NMR (THF): δ 8.66 (s, 1H, O*H*); 7.73 (d, 2h); 7.42 (t, 2H); 7.35 (m, 2H); 7.25 (t, 1H); 6.87 (m, 2H). ^{19}F NMR (THF): δ −137.9 (d, 1F, $^3J_{FF}$ = 131 Hz); −152.3 (d, 1F, $^3J_{FF}$ = 131 Hz). ^{13}C NMR ($CDCl_3$): δ 153.6 (s); 148.2 (dd, $^1J_{CF}$ = 231 Hz, $^2J_{CF}$ = 48 Hz); 146.9 (dd, $^1J_{CF}$ = 240 Hz, $^2J_{CF}$ = 56 Hz); 131.9 (t, J_{CF} = 1.5 Hz, *C*H); 129.7 (t, J_{CF} = 4 Hz, *C*H); 129.5 (d, J_{CF} = 2 Hz, *C*H); 129.4 (dd, J_{CF} = 25 Hz, J_{CF} = 6.5 Hz); 128.7 (d, J_{CF} = 2 Hz, *C*H); 125.9 (dd, J_{CF} = 9 Hz, J_{CF} = 8 Hz, *C*H); 120.8 (s, *C*H); 117.3 (s, *C*H); 116.6 (dd, J_{CF} = 22 Hz, J_{CF} = 4 Hz). Crystals of the complex of phenol **11** with diaza-18-crown-6 suitable for X-ray diffraction were obtained by mixing the ~0.1 M solutions of diaza-18-crown-6 and **11** in dichloromethane. The corresponding phenolates were generated from phenol **11** by the action of *t*-BuOM (M = Li, Na, K) in THF, NaH in toluene and TlOH in THF.

*(E)-2-(1,2-difluoro-2-phenylvinyl)phenolate, (**12**) (o-OMC$_6$H$_4$)CF=CFPh. Sodium salt, M = Na.* ^{19}F NMR (THF): δ −141.0 (d, br., 1F, $^3J_{FF}$ = 129 Hz); −153.8 (d, 1F, $^3J_{FF}$ = 129 Hz). ^{19}F NMR (THF + 18-crown-6): δ −131.1 (d, 1F, $^3J_{FF}$ = 132 Hz); −156.0 (d, 1F, $^3J_{FF}$ = 132 Hz). ^{1}H NMR (THF + 18-crown-6): δ 7.69 (d, 2h); 7.35 (t, 2H); 7.22 (t, 1H); 7.00 (d, 1H); 6.86 (t, 1H); 6.58 (d, 1H); 6.06 (t, 1H). ^{19}F NMR (toluene): δ −143.6 (br., 1F); −153.2 (br., 1F). ^{19}F NMR (toluene + 18-crown-6): δ −131.4 (br., 1F); −156.1 (d, 1F, $^3J_{FF}$ = 129 Hz). *Lithium salt, M = Li.* ^{1}H NMR (THF): δ 7.62 (d, 2h); 7.30 (t, 2H); 7.23 (t, 1H); 7.14 (d, 1H); 6.91 (t, 1H); 6.57 (d, 1H); 6.31 (t, 1H). ^{19}F NMR (THF): δ −139.1 (br., 1F); −155.0 (d, br., 1F, $^3J_{FF}$ = 130 Hz). ^{1}H NMR (THF + 2.2.1-cryptand): δ 7.71 (d, 2h); 7.36 (t, 2H); 7.24 (t, 1H); 7.03 (d, 1H); 6.88 (t, 1H); 6.67 (d, 1H); 6.13 (t, 1H). ^{19}F NMR (THF + 2.2.1-cryptand): δ −133.1 (d, br., 1F, $^3J_{FF}$ = 130 Hz); −155.4 (d, 1F, $^3J_{FF}$ = 130 Hz). *Potassium salt, M = K.* ^{1}H NMR (THF): δ 7.65 (d, 2h); 7.30 (t, 2H); 7.23 (t, 1H); 7.10 (d, 1H); 6.88 (t, 1H); 6.37 (d, 1H); 6.14 (t, 1H). ^{19}F NMR (THF): δ −136.3 (d, 1F, $^3J_{FF}$ = 130 Hz); −154.8 (d, 1F, $^3J_{FF}$ = 130 Hz). ^{1}H NMR (THF + 18-crown-6): δ 7.69 (d, 2h); 7.33 (t, 2H); 7.19 (t, 1H); 6.96 (d, 1H); 6.81 (t, 1H); 6.30 (d, 1H); 5.90 (t, 1H). ^{19}F NMR (THF + 18-crown-6): δ −131.6 (d, 1F, $^3J_{FF}$ = 130 Hz); −156.7 (d, 1F, $^3J_{FF}$ = 130 Hz). *Thallium salt, M = Tl.* ^{1}H NMR (THF): δ 7.69 (d, 2h); 7.39 (t, 2H); 7.32 (m, 2H); 7.19 (t, 1H); 6.84 (d, 1H); 6.75 (t, 1H). ^{19}F NMR (THF): δ −134.9 (d, br., 1F, $^3J_{FF}$ = 130 Hz); −151.7 (d, 1F, $^3J_{FF}$ = 132 Hz).

4.5. NMR data for sodium 1-(2-fluorophenyl)ethoxide

^{1}H NMR (THF): δ 7.76 (m, 1h); 7.05 (m, 2H); 6.86 (m, 1H); 5.39 (q, 1H); 1.34 (d, 3H). ^{19}F NMR (THF): δ −120.3 (m). ^{13}C NMR (THF): δ 161.1 (d, $^1J_{CF}$ = 242 Hz); 143.0 (d, J_{CF} = 16 Hz); 128.0 (s, *C*H); 126.9 (d, J_{CF} = 8 Hz, *C*H); 124.4 (s, *C*H); 114.9 (d, J_{CF} = 23 Hz, *C*H); 66.4 (s, *C*H); 30.1 (s, *C*H$_3$). ^{1}H NMR (THF + 18-crown-6): δ 7.90 (m, 1h); 6.96 (m, 2H); 6.76 (m, 1H); 5.30 (q, 1H); 1.29 (d, 3H). ^{19}F NMR (THF + 18-crown-6): δ −120.3 (m). ^{13}C NMR (THF + 18-crown-6): δ 160.6 (d, $^1J_{CF}$ = 241 Hz); 143.0 (d, J_{CF} = 16 Hz); 129.7 (s, *C*H); 126.3 (d, J_{CF} = 8 Hz, *C*H); 124.1 (s, *C*H); 114.1 (d, J_{CF} = 23 Hz, *C*H); 64.6 (s, *C*H); 29.6 (s, *C*H$_3$).

4.6. X-ray crystal structure determination of 2(11)·(diaza-18-crown-6)

The crystal of 2(**11**)·(diaza-18-crown-6) ($C_{40}H_{46}F_4N_2O_6$, M = 726.79) is triclinic, space group $P\bar{1}$, at T = 173 K: a = 7.7054(15) Å, b = 9.3670(19) Å, c = 13.286(3) Å, α = 99.41(3)°, β = 90.25(3)°, γ = 98.77(3)°, V = 934.6(4) Å^3, Z = 1, d_{calc} = 1.291 g/cm^3, F(0 0 0) = 384, μ = 0.099 mm^{-1}. 3930 total reflections (3641 unique reflections, R_{int} = 0.032) were measured on an automated four-circle diffractometer Syntex P2$_1$ (λ(MoK$_\alpha$)-radiation, graphite monochromator, $\omega/2\theta$ scan mode, $2\theta_{max}$ = 52°). The structure was determined by direct methods and refined by full-matrix least squares technique on F^2 with anisotropic displacement parameters for non-hydrogen atoms. The hydrogen atoms of the hydroxy and amino groups were localized in the difference-Fourier map and included in the refinement with fixed positional and thermal parameters. The other hydrogen atoms were placed in calculated positions and refined within riding model with fixed isotropic displacement parameters [U_{iso}(H) = 1.2U_{eq}(C)]. The final divergence factors were R_1 = 0.059 for 2132 independent reflections with $I > 2\sigma(I)$ and wR_2 = 0.126 for all independent reflections, S = 1.000. All calculations were carried out using the SHELXTL program. [32] Crystallographic data for 2(**11**)·(diaza-18-crown-6) have been deposited with the Cambridge Crystallographic Data Center as supplementary publication no. CCDC 827829. Copies of the data can be obtained, free of charge, on application to CCDC, 12 Union Road, Cambridge CB2 1EZ, UK (fax: +44 1223 336033 or e mail: deposit@ccdc.cam.ac.uk or www.ccdc.cam.ac.uk.

4.7. Computational details

Geometries were optimized with the methods indicated in the corresponding figures and Table 2. Chemical shifts were calculated by GIAO method [33,34] for the structures optimized at the same theory level. All calculations were performed with Gaussian 03 program [35].

Acknowledgements

The authors gratefully acknowledge financial support of this work from the Program of the President of the Russian Federation for the State Support of Leading Research Schools (Grant No. HIII-4365.2010.3). The authors thank Dr. P.A. Khavrel for the help in obtaining the ^{19}F NMR spectra of the Li salt of complex **4**, P&M Company (Moscow) for the gift of chlorotrifluoroethylene and Prof. I.F. Gunkin (Saratov State Technical University) for the gift of metallic thallium.

References

[1] P. Murray-Rust, W.C. Stallings, C.T. Mont, R.K. Preston, J.P. Glusker, J. Am. Chem. Soc. 105 (1983) 3206–3214.
[2] H. Plenio, R. Diodone, Angew. Chem. Int. Ed. 33 (1994) 2175–2177.
[3] H. Plenio, Chem. Rev. 97 (1997) 3363–3384.
[4] H. Plenio, ChemBioChem 5 (2004) 650–655.
[5] H. Plenio, R. Diodone, J. Am. Chem. Soc. 118 (1996) 356–367.
[6] H. Plenio, R. Diodone, Chem. Ber. Recl. 130 (1997) 963–968.
[7] H. Plenio, J. Hermann, R. Diodone, Inorg. Chem. 36 (1997) 5722–5729.
[8] H.J. Buschmann, J. Hermann, M. Kaupp, H. Plenio, Chem. Eur. J. 5 (1999) 2566–2572.
[9] H. Takemura, N. Kon, M. Yasutake, H. Kariyazono, T. Shinmyozu, T. Inazu, Angew. Chem. Int. Ed. 38 (1999) 959–961.
[10] H. Takemura, Curr. Org. Chem. 9 (2005) 521–533.

[11] H. Takemura, H. Kariyazono, M. Yasutake, N. Kon, K. Tani, K. Sako, T. Shinmyozu, T. Inazu, Eur. J. Org. Chem. (2000) 141–148.
[12] H. Takemura, N. Kon, M. Kotoku, S. Nakashima, K. Otsuka, M. Yasutake, T. Shinmyozu, T. Inazu, J. Org. Chem. 66 (2001) 2778–2783.
[13] H. Takemura, S. Nakashima, N. Kon, M. Yasutake, T. Shinmyozu, T. Inazu, J. Am. Chem. Soc. 123 (2001) 9293–9298.
[14] F. Hannig, R. Frohlich, K. Bergander, G. Erker, J.L. Petersen, Organometallics 23 (2004) 4495–4502.
[15] A.R. Siedle, R.A. Newmark, W.M. Lamanna, J.C. Huffman, Organometallics 12 (1993) 1491–1492.
[16] J. Karl, G. Erker, R. Frohlich, J. Am. Chem. Soc. 119 (1997) 11165–11173.
[17] M. Dahlmann, G. Erker, R. Frohlich, O. Meyer, Organometallics 19 (2000) 2956–2967.
[18] M. Hill, G. Kehr, G. Erker, O. Kataeva, R. Fröhlich, Chem. Commun. (2004) 1020–1021.
[19] P.K. Sazonov, G.A. Artamkina, K.A. Lyssenko, I.P. Beletskaya, J. Organomet. Chem. 691 (2006) 2346–2357.
[20] K.P. Darst, C.M. Lukehart, J. Organomet. Chem. 171 (1979) 65–71.
[21] V.A. Ivushkin, P.K. Sazonov, G.A. Artamkina, I.P. Beletskaya, J. Organomet. Chem. 597 (2000) 77–86.
[22] C.P. Casey, D.M. Scheck, J. Am. Chem. Soc. 102 (1980) 2723–2728.
[23] P.K. Sazonov, G.A. Artamkina, V.N. Khrustalev, M.Y. Antipin, I.P. Beletskaya, J. Organomet. Chem. 681 (2003) 59–69.
[24] C.P. Casey, C.J. Czerwinski, R.K. Hayashi, Organometallics 15 (1996) 4362–4365.
[25] P.K. Sazonov, G.A. Artamkina, I.P. Beletskaya, Russ. J. Org. Chem. 36 (2000) 943–950.
[26] P.K. Sazonov, M.M. Shtern, G.A. Artamkina, I.P. Beletskaya, Russ. J. Org. Chem. 34 (1998) 1736–1749.
[27] P.K. Sazonov, L.K. Minacheva, A.V. Churakov, V.S. Sergienko, G.A. Artamkina, Y.F. Oprunenko, I.P. Beletskaya, Dalton Trans. (2009) 843–850.
[28] D. Andrae, U. Haeussermann, M. Dolg, H. Stoll, H. Preuss, Theor. Chim. Acta 77 (1990) 123.
[29] F.H. Allen, Acta Crystallogr. B58 (2002) 380–388.
[30] K. Mikami, Chem. Rec. 6 (2006) 1–11.
[31] H. Takemura, M. Kaneko, K. Sakob, T. Iwanagac, New J. Chem. 33 (2009) 2004–2006.
[32] G.M. Sheldrick, Acta Crystallogr. A64 (2008) 112–122.
[33] R. Ditchfield, Mol. Phys. 27 (1974) 789–807.
[34] K. Wolinski, J.F. Hinton, P. Pulay, J. Am. Ceram. Soc. 112 (1990) 8251–8260.
[35] M.J. Frisch, G.W. Trucks, H.B. Schlegel, G.E. Scuseria, M.A. Robb, J.R. Cheeseman, J.A. Montgomery, J.T. Vreven, K.N. Kudin, J.C. Burant, J.M. Millam, S.S. Iyengar, J. Tomasi, V. Barone, B. Mennucci, M. Cossi, G. Scalmani, N. Rega, G.A. Petersson, H. Nakatsuji, M. Hada, M. Ehara, K. Toyota, R. Fukuda, J. Hasegawa, M. Ishida, T. Nakajima, Y. Honda, O. Kitao, H. Nakai, M. Klene, X. Li, J.E. Knox, H.P. Hratchian, J.B. Cross, C. Adamo, J. Jaramillo, R. Gomperts, R.E. Stratmann, O. Yazyev, A.J. Austin, R. Cammi, C. Pomelli, J.W. Ochterski, P.Y. Ayala, K. Morokuma, G.A. Voth, P. Salvador, J.J. Dannenberg, V.G. Zakrzewski, S. Dapprich, A.D. Daniels, M.C. Strain, O. Farkas, D.K. Malick, A.D. Rabuck, K. Raghavachari, J.B. Foresman, J.V. Ortiz, Q. Cui, A.G. Baboul, S. Clifford, J. Cioslowski, B.B. Stefanov, G. Liu, A. Liashenko, P. Piskorz, I. Komaromi, R.L. Martin, D.J. Fox, T. Keith, M.A. Al-Laham, C.Y. Peng, A. Nanayakkara, M. Challacombe, P.M.W. Gill, B. Johnson, W. Chen, M.W. Wong, C. Gonzalez, J.A. Pople, Gaussian 03, Revision C.01, Gaussian, Inc., Pittsburgh PA, 2003.